IEICE TRANSACTIONS

on Fundamentals of Electronics, Communications and Computer Sciences

DOI:10.1587/transfun.2024EAP1037

Publicized:2024/09/09

A PUBLICATION OF THE ENGINEERING SCIENCES SOCIETY

The Institute of Electronics, Information and Communication Engineers

Kikai-Shinko-Kaikan Bldg., 5-8, Shibakoen 3 chome, Minato-ku, TOKYO, 105-0011 JAPAN

PAPER

Thinned Waveform Design of MIMO Radar in Interference Environment

Mingjie LIU[†a)], Chunyang WANG[†], Jian GONG[†b)], Ming TAN[††], *and* Changlin ZHOU[†], *Nomembers*

SUMMARY To improve multiple input multiple output (MIMO) radar performance and reduce computation complexity, we propose a thinned waveform design algorithm. We form an optimization problem, which the objective function is combined with signal-to-interference-and-noise-ratio (SINR) and Cramer-Rao lower bound (CRLB). Waveform code, waveform selection and antenna selection can be as optimization variables. We define the waveform code-antenna selection vector, which can denote waveform code and antenna simultaneous selection. Due to the problem is multivariate non-convex optimization, we propose a sequential iterative optimization algorithm. The problem is decomposed into two subproblems about waveform code and code-antenna selection vector. To optimize the code-antenna selection vector, we transform the optimization problem into a conventional convex problem by logarithms and first-order Taylor expansions. For waveform code optimization, we introduced an auxiliary variable and solved it by Alternating Direction Method of Multipliers (ADMM). Convex (CVX) can solve the subproblems. The simulation result shows that the better performance and lower computation complexity by the proposed approach than other methods.

key words: *multiple input multiple output (MIMO) radar ; thinned waveform design ; signal-to-interference-and-noise-ratio (SINR) ; Cramer-Rao lower bound (CRLB)*

1. Introduction

Multiple Input and Multiple Output (MIMO) has excellent performance in many aspects, such as target detection, parameter estimation, radio frequency stealth, and anti-interference[1, 2].

Compared with the uniform MIMO, the sparse MIMO has lower mutual coupling and significant advantages in reducing cost and data computation[3-8]. It can also provide high-resolution parameter estimation and process more sources than physical sensors[9-12]. Many researchers have studied various sparse array, including nested arrays, coprime arrays, etc. However, some scholars believe that the optimal sparse array configuration is the array that has high output signal-to-noise-ratio(SNR). [13-17] research the unstructured sparse arrays. It can adaptively adjust the array structure with the interference environment. [16] introduce antenna-pulse selection vector, proposing a novel thinned (space-time adaptive processing)STAP by selecting an optimum subset of antenna-pulse code pairs that achieves the maximum output signal-to-clutter-plus-noise-ratio. However, [16] did not consider pulse code design. The waveform code design can make MIMO radar processing more flexible. It can provide MIMO radar with more capabilities, especially anti-interference[18-20]. To further improve signal-to-interference-and-noise-ratio(SINR), waveform degrees of freedom can be utilized. [21] focused on the waveform design for radar and the extended target in the environment of electronic warfare. [22] develop and present a radar waveform design method that optimizes the spectral shape of the radar waveform. [23] proposed a new approach based on a Riemannian manifold. [24-26] focus on improving target detection capability in the presence of interference, proposing design method of transmit waveform.

The signal dimension may be large for large scale MIMO. Some researchers researched the thinned waveform design, which it can be also called as the joint design of waveforms and antenna selection[27-32]. [27] aim low system overhead and radar-communication dual function, proposing a switchable individual antenna power control scheme to optimize waveforms and antenna locations jointly. [29] investigate the joint optimization of the waveform covariance matrix and the antenna position vector for a MIMO radar system to approximate some index. And, in order to further reduce the data volume of the sensing system signal processing, [31] proposed a waveform optimization design method and target parameter estimation technique for a compressed sensing MIMO radar based on a 2D antenna array.

In this paper, we consider MIMO radar performance and system complexity. We proposed a thinned waveform design approach in the interference environment, which is the waveform code-antenna selection and discrete code design. We combine SINR and Cramer-Rao lower bound (CRLB) to form function representing radar performance by introducing code-antenna selection vector $\mathbf{z}$ and code waveform $\mathbf{x}$. Then, we form optimization problems with the new function and constraints to improve radar performance. Because of multivariate non-convex optimization problems, we proposed a sequential iterative optimization algorithm. We decompose the problem into two subproblems. They are about the problem of $\mathbf{z}$ and $\mathbf{x}$, respectively. For the optimization of $\mathbf{z}$, we transform the optimization problem into a conventional convex problem by logarithms and first-order Taylor expansions. For optimization of $\mathbf{x}$, we introduced an auxiliary variable and solved it by Alternating

†The author is with Air and Missile Defense College, Air Force Engineering University, Xi'an 710051, China
††The author is with School of information and communication, National University of Defense Technology, Wuhan 430019, China.
a) E-mail: Lmjie09@aliyun.com
b) E-mail: drgong@aliyun.com

Direction Method of Multipliers(ADMM). The convex(CVX) toolbox can solve the subproblems. Finally, we take some simulations. The simulation result shows that MIMO radar has good performance and low complexity by the proposed approach.

2. MIMO Signal model

Consider a collocated narrow band MIMO radar, system, as shown in Fig. 1, the MIMO radar has N transmit antennas and M receive antennas. The interelement space is d.

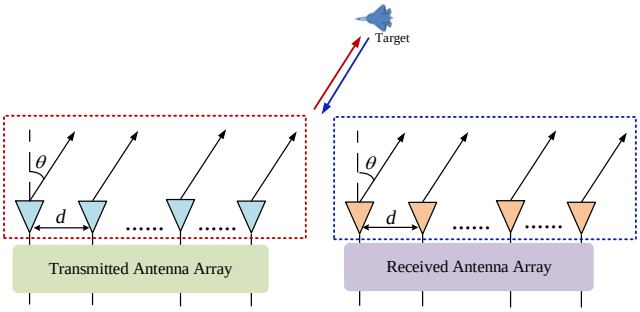

Fig. 1 Collocated MIMO radar.

Each transmit antenna transmits different waveform code. The signal of the n-th transmit antenna is $\mathbf{x}_n$, n=1, 2, ⋯, N. $\mathbf{x}_n = [x_n(1), x_n(2), \cdots, x_n(L)]$. $x_n(l)$ is the l-th signal code, l=1, 2, ⋯, L, L is the number of time samples. Suppose one desired signal and J interference signals impinge on the array from J+1 narrowband far-field sources. The signal received by the array is modeled as

$$\mathbf{R} = \zeta_0 \mathbf{b}(\theta_0)\mathbf{a}^T(\theta_0)\mathbf{X} + \sum_{j=1}^{J} \zeta_j \mathbf{b}(\theta_j)\mathbf{a}^T(\theta_j)\mathbf{X}_j + \mathbf{N} \quad (1)$$

where $\mathbf{R} = \left[\mathbf{r}_1^T, \cdots, \mathbf{r}_M^T\right]^T$, $\mathbf{r}_m \in \mathbb{C}^{1\times L}$ is the received signal of the m-th received array element, m=1,2, ⋯, M. $\mathbf{X} = \left[\mathbf{x}_1^T, \cdots, \mathbf{x}_N^T\right]^T$, is desired signal code matrix, $\mathbf{X} \in \mathbb{C}^{N\times L}$. $\mathbf{X}_j$ is interference signal code matrix, which interference is radar signal-dependent, it can also be considered as $\mathbf{X}_j = \mathbf{X}$. $\mathbf{N} = \left[\mathbf{n}_1^T, \cdots, \mathbf{n}_M^T\right]^T$ is a complex white Gaussian noise matrix with zero mean, and it is uncorrelated with the desired signal and interference signal. ζ_0 and ζ_j are amplitude of desired signal and interference signal, $\mathbf{a}(\theta) \in \mathbb{C}^{N\times 1}$ and $\mathbf{b}(\theta) \in \mathbb{C}^{N\times 1}$ are transmit steering vector and receive steering vector, respectively. They can be written as

$$\mathbf{a}(\theta) = \left[1, e^{j2\pi\frac{f_0 d\sin\theta}{c}}, \cdots, e^{j2\pi(N-1)\frac{f_0 d\sin\theta}{c}}\right]^T \quad (2)$$

$$\mathbf{b}(\theta) = \left[1, e^{j2\pi\frac{f_0 d\sin\theta}{c}}, \cdots, e^{j2\pi(M-1)\frac{f_0 d\sin\theta}{c}}\right]^T \quad (3)$$

where f_0 is carrier frequency, d is inter-element space, c is electromagnetic wave propagation speed.

We vectorize model (1). The ML-dimensional received complex-valued vector can be expressed as

$$\mathbf{r} = \zeta_0 \mathbf{A}(\theta_0)\mathbf{x} + \sum_{j=1}^{J} \zeta_j \mathbf{A}(\theta_j)\mathbf{x}_j + \mathbf{n} \quad (4)$$

where $\mathbf{r} = vec\{\mathbf{R}\} \in \mathbb{C}^{ML\times 1}$, $\mathbf{x} = vec\{\mathbf{X}\} \in \mathbb{C}^{NL\times 1}$, $\mathbf{x}_j = vec\{\mathbf{X}_j\} \in \mathbb{C}^{NL\times 1}$, $\mathbf{n} = vec\{\mathbf{N}\} \in \mathbb{C}^{ML\times 1}$, $\mathbf{A}(\theta_0)$ and $\mathbf{A}(\theta_j)$ are steering matrix of desired signal and interference signal, $\mathbf{A}(\theta) = \mathbf{I}_L \otimes \left[\mathbf{b}(\theta)\mathbf{a}^T(\theta)\right]$, $\mathbf{A}(\theta) \in \mathbb{C}^{ML\times NL}$.

3. MIMO Radar Thinned Waveform Design

3.1 Output SINR and CRLB

3.1.1. Output SINR

Minimum variance distortionless response(MVDR) is an adaptive beamforming algorithm based on the maximum SINR criterion. The MVDR algorithm can adaptively minimize the power of the array output in the desired direction and maximize the SINR. The optimum weight vector $\mathbf{w}$ for minimizing the output variance while keeping the desired signal distortionless can be expressed as the following optimization problem

$$\begin{aligned} &\min_{\mathbf{w}} \ \mathbf{w}^H \mathbf{R}_{j+n} \mathbf{w} \\ &\text{s.t.} \ \ \mathbf{w}^H \mathbf{R}_s \mathbf{w} = 1. \end{aligned} \quad (5)$$

where $\mathbf{R}_{j+n}$ is the interference and noise covariance matrix. $\mathbf{R}_s$ is the received signal covariance matrix.

By solving the optimal weight vector, we can obtain the SINR.

$$\begin{aligned} \text{SINR} &= \zeta_0^2 \frac{\mathbf{w}_{opt}^H \mathbf{s}\mathbf{s}^H \mathbf{w}_{opt}}{\mathbf{w}_{opt}^H \mathbf{R}_{j+n}^{-1} \mathbf{w}_{opt}} \\ &= \zeta_0^2 \mathbf{s}^H \mathbf{R}_{j+n}^{-1} \mathbf{s} \end{aligned} \quad (6)$$

where $\mathbf{R}_{j+n} = \sum_{j=1}^{J} \zeta_j^2 \mathbf{A}(\theta_j)\mathbf{x}\mathbf{x}^H \mathbf{A}(\theta_j)^H + \mathbf{n}\mathbf{n}^H$, ζ_0 is echo signal amplitude, ζ_j is the j-th interference amplitude.

We define $\mathbf{s}$ as a waveform-steering vector of target, $\mathbf{s} = \mathbf{A}(\theta_0)\mathbf{x} = \left\{\mathbf{I}_L \otimes \left[\mathbf{b}(\theta_0)\mathbf{a}^T(\theta_0)\right]\right\}\mathbf{x}$. The SINR also can be written as

$$\begin{aligned} \text{SINR} = \zeta_0^2 \mathbf{x}^H &\left\{\mathbf{I}_L \otimes \left[\mathbf{b}(\theta_0)\mathbf{a}^T(\theta_0)\right]\right\}^H \\ &\times \mathbf{R}_{j+n}^{-1} \left\{\mathbf{I}_L \otimes \left[\mathbf{b}(\theta_0)\mathbf{a}^T(\theta_0)\right]\right\}\mathbf{x} \end{aligned} \quad (7)$$

We can conclude from (7) that SINR is related to $\mathbf{A}(\theta_0)$ and $\mathbf{x}$.

The output SINR also can be written as another expression. According to the matrix inversion lemma, the interference noise inverse covariance matrix can be written

as

$$\mathbf{R}_{j+n}^{-1}=\sigma^{-2}\left(\mathbf{I}-\mathbf{S}_j\left(\mathbf{C}_j+\mathbf{S}_j^H\mathbf{S}_j\right)^{-1}\mathbf{S}_j^H\right) \tag{8}$$

where $\mathbf{C}_j=\sigma^2\mathbf{C}_v$, $\mathbf{C}_v=E\left\{\mathbf{x}_j\mathbf{x}_j^H\right\}$, σ is noise standard deviation, $\mathbf{S}_j=\left[\mathbf{s}_1^T,\cdots,\mathbf{s}_J^T\right]^T$, $\mathbf{s}_j$ is the interference waveform-steering vector. We substitute (8) into (6), the output SINR also can be written as

$$\begin{aligned}\mathrm{SINR}&=\mathrm{SNR}\bullet\mathbf{s}^H\left(\mathbf{I}-\mathbf{S}_j\left(\mathbf{C}_j+\mathbf{S}_j^H\mathbf{S}_j\right)^{-1}\mathbf{S}_j^H\right)\mathbf{s}\\&=\mathrm{SNR}\frac{\left|\bar{\mathbf{S}}^H\bar{\mathbf{S}}+\mathbf{C}\right|}{\left|\mathbf{S}_j^H\mathbf{S}_j+\mathbf{C}_j\right|}\end{aligned} \tag{9}$$

where $\bar{\mathbf{S}}=\left[\mathbf{s},\ \mathbf{S}_j\right]$, $\mathbf{C}$ is the augmented interference covariance matrix

$$\mathbf{C}=\begin{bmatrix}0 & \mathbf{0}_{1\times J}\\ \mathbf{0}_{J\times 1} & \mathbf{C}_j\end{bmatrix} \tag{10}$$

3.1.2. CRLB

Due to noise, radar cannot estimate target parameters without any error. The Cramer-Rao Lower Bound gives a lower limit to the standard deviation of any unbiased parameter estimation. CRLB reflects the radar performance in parameter estimation.

CRLB can be obtained by inverting the Fisher information matrix. We only consider the direction of arrival estimation, Fishler information is

$$f=2\mathrm{Re}\left[\frac{\partial\boldsymbol{\mu}^H}{\partial\theta_0}\mathbf{R}_n^{-1}\frac{\partial\boldsymbol{\mu}}{\partial\theta_0}\right] \tag{11}$$

where $\boldsymbol{\mu}=\zeta_0\left\{\mathbf{I}_L\otimes\left[\mathbf{b}(\theta_0)\mathbf{a}^T(\theta_0)\right]\right\}\mathbf{x}$, $\mathbf{R}_n^{-1}$ is noise covariance matrix inverse, $\mathbf{R}_n^{-1}=\sigma^{-2}\mathbf{I}_{NL\times NL}$ in this paper. Assuming that the inter-elements spacing between the transmit and receive array both are half wavelength, $\frac{\partial\boldsymbol{\mu}}{\partial\theta_0}$ can be written as

$$\begin{aligned}\frac{\partial\boldsymbol{\mu}}{\partial\theta_0}=\zeta_0\Bigg\{\mathbf{I}_L\otimes\Bigg[&-j2\pi f_0\frac{d\cos(\theta_0)}{c}\\&\times\left(\mathbf{D}_m\mathbf{b}(\theta_0)\mathbf{a}^T(\theta_0)+\mathbf{b}(\theta_0)\mathbf{a}^T(\theta_0)\mathbf{D}_n\right)\Bigg]\Bigg\}\mathbf{x}\end{aligned} \tag{12}$$

where $\mathbf{D}_m=diag\left\{0,1,\cdots,M-1\right\}$, $\mathbf{D}_n=diag\left\{0,1,\cdots,N-1\right\}$.

$$\begin{aligned}f=\ &2\mathrm{SNR}\pi^2\cos^2(\theta_0)\mathbf{x}^H\left\{\mathbf{I}_L\otimes\left[\left(\mathbf{D}_m\mathbf{b}(\theta_0)\mathbf{a}^T(\theta_0)+\mathbf{b}(\theta_0)\mathbf{a}^T(\theta_0)\mathbf{D}_n\right)\right]\right\}^H\\&\times\left\{\mathbf{I}_L\otimes\left[\left(\mathbf{D}_m\mathbf{b}(\theta_0)\mathbf{a}^T(\theta_0)+\mathbf{b}(\theta_0)\mathbf{a}^T(\theta_0)\mathbf{D}_n\right)\right]\right\}\mathbf{x}\end{aligned} \tag{13}$$

3.1.3. Thinned Waveform

[13] introduce the unstructured arrays design. We can also introduce waveform code selection vector to reduce the array complexity. If there are Q possible waveform code and K available code, we can suppose that that the waveform code selection vector is $\mathbf{z}=\left[z_i,i=1,\cdots,Q\right]\in\left\{0,1\right\}^Q$. When $z_i=0$, it denotes the waveform code is not selected, and $z_i=1$ denotes the waveform code is selected. There is a corresponding selection matrix $\mathbf{Z}\in\left\{0,1\right\}^{K\times Q}$ with $z_{ij}=1$ in the i-th row and the j-th column, where $i=1,\cdots,K$ and $j\in\left\{1,\cdots,Q\right\}$. The selection vector $\mathbf{z}$ and selection matrix $\mathbf{Z}$ are inner-connected by $\mathbf{Z}^T\mathbf{Z}=diag(\mathbf{z})$. The diagonal matrix $diag(\mathbf{z})$ is the waveform code selection operator with the vector $\mathbf{z}$ populating along the diagonal. The target waveform-steering vector and interference waveform-steering vector after code selection can be written as $\mathbf{Zs}$ and $\mathbf{ZV}$, respectively.

Based on the discussion, the received signal model with thinned waveform code is

$$\mathbf{r}_\mathbf{z}=\zeta_0\mathbf{ZA}\left(\theta_0\right)\mathbf{x}+\sum_{j=1}^{J}\zeta_j\mathbf{ZA}\left(\theta_j\right)\mathbf{x}+\mathbf{n}_\mathbf{z} \tag{14}$$

where $\mathbf{r}_\mathbf{z}\in\mathbb{C}^{K\times 1}$, $\mathbf{n}_\mathbf{z}\in\mathbb{C}^{K\times 1}$, $\mathbf{Z}\in\left\{0,1\right\}^{K\times ML}$, $\mathbf{r}_\mathbf{z}$ is the received signal after selection, $\mathbf{n}_\mathbf{z}$ is the noise after selection.

And then, $\mathbf{R}_{j+n}$ can be expressed as

$$\mathbf{R}_{j+n}=\sum_{j=1}^{J}\zeta_j^2\mathbf{ZA}\left(\theta_j\right)\mathbf{x}\mathbf{x}^H\mathbf{A}\left(\theta_j\right)^H\mathbf{Z}^H+\mathbf{n}_\mathbf{z}\mathbf{n}_\mathbf{z}^H \tag{15}$$

After introducing the waveform code selection vector, the SINR and CRLB can be expressed as

$$\begin{aligned}\mathrm{SINR}&=\mathrm{SNR}\frac{\left|\bar{\mathbf{S}}^H diag(\mathbf{z})\bar{\mathbf{S}}+\mathbf{C}\right|}{\left|\mathbf{S}_j^H diag(\mathbf{z})\mathbf{S}_j+\mathbf{C}_j\right|}\\&=\zeta_0^2\mathbf{x}^H\mathbf{A}(\theta_0)^H\mathbf{Z}^H\mathbf{R}_{j+n}^{-1}\mathbf{ZA}(\theta_0)\mathbf{x}\end{aligned} \tag{16}$$

$$\begin{aligned}f=\ &4\mathrm{SNR}\pi^2\cos^2(\theta_0)\\&\times\mathbf{x}^H\left\{\mathbf{I}_L\otimes\left[\left(\mathbf{D}_m\mathbf{b}(\theta_0)\mathbf{a}^T(\theta_0)+\mathbf{b}(\theta_0)\mathbf{a}^T(\theta_0)\mathbf{D}_n\right)^H\right.\right.\\&\left.\left.\times diag(\mathbf{z})\left(\mathbf{D}_m\mathbf{b}(\theta_0)\mathbf{a}^T(\theta_0)+\mathbf{b}(\theta_0)\mathbf{a}^T(\theta_0)\mathbf{D}_n\right)\right]\right\}\mathbf{x}\end{aligned} \tag{17}$$

3.2. Thinned Waveform Design

To balance SINR and CRLB, we introduce pareto weight, μ ($0\le\mu\le 1$). And we write it as expressions for $\mathbf{x}$ and $\mathbf{z}$, respectively.

$$\begin{aligned} F(\mathbf{x},\mathbf{z}) &= (1-\mu)\varepsilon_1 \mathrm{SINR} + \mu\varepsilon_2 f \\ &= (1-\mu)\varepsilon_1 \mathbf{x}^H \mathbf{A}(\theta_0)^H \mathbf{Z}^H \mathbf{R}_{j+n}^{-1} \mathbf{Z}\mathbf{A}(\theta_0)\mathbf{x} + \mu\varepsilon_2 \mathbf{x}^H \Xi(\mathbf{z})\mathbf{x} \\ &= (1-\mu)\varepsilon_1 \frac{\left|\bar{\mathbf{S}}^H diag(\mathbf{z})\bar{\mathbf{S}} + \mathbf{C}\right|}{\left|\mathbf{S}_j^H diag(\mathbf{z})\mathbf{S}_j + \mathbf{C}_j\right|} + \mu\varepsilon_2 \mathbf{x}^H \left\{\mathbf{I}_L \otimes \left[\Psi^H diag(\mathbf{z})\Psi\right]\right\}\mathbf{x} \end{aligned} \tag{18}$$

where $\Xi(\mathbf{z}) = \mathbf{I}_L \otimes \left[\Psi^H diag(\mathbf{z})\Psi\right]$, $\Psi = \mathbf{D}_m \mathbf{b}(\theta)\mathbf{a}^T(\theta) + \mathbf{b}(\theta)\mathbf{a}^T(\theta)\mathbf{D}_n$, ε_1, ε_2 are fixed value, which are the adjustment coefficient for adjusting the proportion of SINR and CRLB optimization values, respectively.

To improve the radar performance, we establish an optimization problem that maximizes $F(\mathbf{x}, \mathbf{z})$. We consider avoiding the transmitted signal distortions when high power amplifiers work in near saturation mode. We consider the constant modulus constraint on the waveforms. We assume K available code. The optimization problem can be formulated as

$$\begin{aligned} \max \quad & F(\mathbf{x},\mathbf{z}) \\ s.t. \quad & \mathbf{x}^H\mathbf{x} = 1 \\ & \|\mathbf{z}\|_0 = K \\ & \mathbf{z} \in \{0,1\}^{NL} \end{aligned} \tag{19}$$

We can see that (19) is a multivariate non-convex problem. It is challenging to solve for $\mathbf{x}$ and $\mathbf{z}$. Therefore, we propose a sequential iterative optimization algorithm. We decompose (19) into two subproblems. They are about the problem of $\mathbf{z}$ and $\mathbf{x}$, respectively.

3.2.1. Optimization of $\mathbf{z}$

For a fixed waveform code $\mathbf{x}$, the optimal $\mathbf{z}$ can be obtained by rewriting (19) as

$$\begin{aligned} \max_{\mathbf{z}\in\mathbb{R}^{ML}} \quad & F(\mathbf{z}) \\ \text{s.t.} \quad & \|\mathbf{z}\|_0 = K \\ & \mathbf{z} \in \{0,1\}^{ML}. \end{aligned} \tag{20}$$

Taking the logarithm of $\left|\bar{\mathbf{B}}^H diag(\mathbf{z})\bar{\mathbf{B}} + \mathbf{C}\right| \Big/ \left|\mathbf{B}^H diag(\mathbf{z})\mathbf{B} + \mathbf{C}_j\right|$, We can get

$$\begin{aligned} F' = (1-\mu)\varepsilon_1 \Big(&\log\left|\bar{\mathbf{B}}^H diag(\mathbf{z})\bar{\mathbf{B}} + \mathbf{C}\right| \\ &- \log\left|\mathbf{B}^H diag(\mathbf{z})\mathbf{B} + \mathbf{C}_j\right|\Big) \\ &+ \mu\varepsilon_2 \mathbf{x}^H \left\{\mathbf{I}_L \otimes \left[\Psi^H diag(\mathbf{z})\Psi\right]\right\}\mathbf{x} \end{aligned} \tag{21}$$

Because of $\left|\bar{\mathbf{B}}^H diag(\mathbf{z})\bar{\mathbf{B}} + \mathbf{C}\right| \Big/ \left|\mathbf{B}^H diag(\mathbf{z})\mathbf{B} + \mathbf{C}_j\right|$ and logarithm operation, $F' < F$. For the (20), maximizing F is equivalent to maximizing the lower bound of F, F'. And we transform the maximization problem into a minimization problem. We can get that

$$\begin{aligned} \min_{\mathbf{z}\in\mathbb{R}^{NxL}} \quad & -(1-\mu)\varepsilon_1 \Big(\log\left|\bar{\mathbf{B}}^H diag(\mathbf{z})\bar{\mathbf{B}} + \mathbf{C}\right| \\ & - \log\left|\mathbf{B}^H diag(\mathbf{z})\mathbf{B} + \mathbf{C}_j\right|\Big) \\ & - \mu\varepsilon_2 \mathbf{x}^H \left\{\mathbf{I}_L \otimes \left[\Psi^H diag(\mathbf{z})\Psi\right]\right\}\mathbf{x} \\ \text{s.t.} \quad & \|\mathbf{z}\|_0 = K \\ & \mathbf{z} \in \{0,1\}^N. \end{aligned} \tag{22}$$

It is difficult to solve (35) due to the non-convex objective function and the constraints. Fortunately, the non-convex problem can be converted to a series of convex subproblems by sequential convex programming(SCP), which is based on iteratively linearizing the concave function $\log\left|\bar{\mathbf{B}}^H diag(\mathbf{z})\bar{\mathbf{B}} + \mathbf{C}\right|$. Utilizing the first-order Taylor series to expand the concave function. We can get the problem

$$\begin{aligned} \min_{\mathbf{z}\in\mathbb{R}^{ML}} \quad & (1-\mu)\varepsilon_1 \Big(\nabla f\left(\mathbf{z}^{(k)}\right)^T \left(\mathbf{z} - \mathbf{z}^{(k)}\right) \\ & - \log\left|\bar{\mathbf{B}}^H diag(\mathbf{z})\bar{\mathbf{B}} + \mathbf{C}\right|\Big) \\ & - \mu\varepsilon_2 \mathbf{x}^H \left\{\mathbf{I}_L \otimes \left[\Psi^H diag(\mathbf{z})\Psi\right]\right\}\mathbf{x} \\ \text{s.t.} \quad & \mathbf{1}^T\mathbf{z} = K, \\ & 0 \le \mathbf{z} \le 1. \end{aligned} \tag{23}$$

where $\nabla f\left(\mathbf{z}^{(k)}\right)$ represents the gradient of $\log\left|\bar{\mathbf{B}}^H diag(\mathbf{z})\bar{\mathbf{B}} + \mathbf{C}\right|$ around $\mathbf{z}^{(k)}$. The i-th element of $\nabla f\left(\mathbf{z}^{(k)}\right)$ is

$$\begin{aligned} &\left[\nabla f\left(\mathbf{z}^{(k)}\right)\right]_i = \\ &\mathbf{b}_i^H \left(\mathbf{B}^H diag\left(\mathbf{z}^{(k)}\right)\mathbf{B} + \sigma_n^2 \Lambda^{-1}\right)^{-1} \mathbf{b}_i \end{aligned} \tag{24}$$

We can solve the problem (23) by CVX. The final antenna selection vector is achieved by setting the largest K elements of $\mathbf{z}$ to one.

3.2.2. Optimization of $\mathbf{x}$

After obtaining the waveform code selection vector $\mathbf{z}$, we can obtain $\mathbf{Z}$ by $\mathbf{z}$. Then, the optimal $\mathbf{x}$ can be obtained by rewriting (19) as

$$\begin{aligned} \max_{\mathbf{x}} \quad & (1-\mu)\varepsilon_1 \mathbf{x}^H \mathbf{A}(\theta_0)^H \mathbf{Z}^H \mathbf{R}_{j+n}^{-1} \mathbf{Z}\mathbf{A}(\theta_0)\mathbf{x} \\ & + \mu\varepsilon_2 \mathbf{x}^H \Xi(\mathbf{z})\mathbf{x} \\ \text{s.t.} \quad & \mathbf{x}^H\mathbf{x} = 1. \end{aligned} \tag{25}$$

It can be seen that problem (25) containing a non-convex objective function, nonlinear equality constraints, is non-convex.

An auxiliary variable $\mathbf{h}$ can be introduced to reformulate (25) as

$$\begin{aligned}\min_{\mathbf{s},\mathbf{h}}\ & -(1-\mu)\varepsilon_1\mathbf{x}^H\mathbf{A}(\theta_0)^H\mathbf{Z}^H\mathbf{R}_{j+n}^{-1}\mathbf{Z}\mathbf{A}(\theta_0)\mathbf{h}\\ & -\mu\varepsilon_2\mathbf{x}^H\Xi(\mathbf{z})\mathbf{h}\\ \text{s.t.}\quad & \mathbf{x}^H\mathbf{h}=1\\ & \mathbf{x}-\mathbf{h}=\mathbf{0}.\end{aligned}\tag{26}$$

As shown in the (26), by introducing auxiliary variable $\mathbf{h}$, (26) has become a convex problem. We can solve this problem by using the ADMM algorithm.

Firstly, the scaled augmented Lagrangian function of the problem (26) is formed as

$$\begin{aligned}&L(\mathbf{x},\mathbf{h},u_1,\mathbf{u}_2)\\ &=-(1-\mu)\varepsilon_1\mathbf{x}^H\mathbf{A}(\theta_0)^H\mathbf{Z}^H\mathbf{R}_{j+n}^{-1}\mathbf{Z}\mathbf{A}(\theta_0)\mathbf{h}\\ &\quad-\mu\varepsilon_2\mathbf{x}^H\Xi(\mathbf{z})\mathbf{h}+\frac{\rho_1}{2}\left\|\mathbf{x}^H\mathbf{h}-1+u_1\right\|_2^2\\ &\quad+\frac{\rho_2}{2}\left\|\mathbf{x}-\mathbf{h}+\mathbf{u}_2\right\|_2^2\end{aligned}\tag{27}$$

At the k+1-th iteration, ADMM consists of the following update procedures:

$$\mathbf{x}^{k+1}=\arg\min\left\{\begin{array}{l}-(1-\mu)\varepsilon_1\mathbf{x}^H\mathbf{A}(\theta_0)^H\mathbf{Z}^H\mathbf{R}_{j+n}^{-1}\mathbf{Z}\mathbf{A}(\theta_0)\mathbf{h}^k-\mu\varepsilon_2\mathbf{x}^H\Xi(\mathbf{z})\mathbf{h}^k\\ +\dfrac{\rho_1}{2}\left\|\mathbf{x}^H\mathbf{h}^k-1+u_1^k\right\|_2^2+\dfrac{\rho_2}{2}\left\|\mathbf{x}-\mathbf{h}^k+\mathbf{u}_2^k\right\|_2^2\end{array}\right\}\tag{28}$$

$$\mathbf{h}^{k+1}=\arg\min\left\{\begin{array}{l}-(1-\mu)\varepsilon_1\left(\mathbf{x}^{k+1}\right)^H\mathbf{A}(\theta_0)^H\mathbf{Z}^H\mathbf{R}_{j+n}^{-1}\mathbf{Z}\mathbf{A}(\theta_0)\mathbf{h}-\mu\varepsilon_2\left(\mathbf{x}^{k+1}\right)^H\Xi(\mathbf{z})\mathbf{h}\\ +\dfrac{\rho_1}{2}\left\|\left(\mathbf{x}^{k+1}\right)^H\mathbf{h}-1+u_1^k\right\|_2^2+\dfrac{\rho_2}{2}\left\|\mathbf{x}^{k+1}-\mathbf{h}+\mathbf{u}_2^k\right\|_2^2\end{array}\right\}\tag{29}$$

$$u_1^{k+1}=u_1^k+\left((\mathbf{x}^{k+1})^H\mathbf{h}^{k+1}-1\right)\tag{30}$$

$$\mathbf{u}_2^{k+1}=\mathbf{u}_2^k+\mathbf{x}^{k+1}-\mathbf{h}^{k+1}\tag{31}$$

Based on the aforementioned discussion, the proposed sequential iterative optimization algorithm for the problem (19) is summarized in Table 1.

Note that the optimization result is largely affected by the initial point. In practice, we usually initialize the algorithm with multiple feasible points and find the solution with the minimum objective function value among all the trials.

Table 1 The proposed sequential iterative optimization algorithm.

Algorithm The proposed sequential iterative optimization algorithm

1: Initialize $\mathbf{x}^{(0)}$, iteration stop criteria δ, maximum number of iterations $i_{\max}$, i=0.

2: Set $i=i+1$. Substitute $\mathbf{x}^{(i)}$ into (20). Obtain the $\mathbf{z}^{(i)}$ by solving problem (23).

3: Compute $\mathbf{Z}^{(i)}$ by $\mathbf{z}^{(i)}$, and compute $\mathbf{R}_{j+n}^{(i)}$ by (15).

4: Substitute $\mathbf{Z}^{(i)}$ and $\mathbf{R}_{j+n}^{(i)}$ into (25). Obtain the $\mathbf{x}^{(i)}$ by (28)~(31).

5: Compute $\beta^{(i)}=F^{(i)}-F^{(i-1)}$ by (18).

6: If $i\ge i_{\max}$ or $\beta^{(i)}<\delta$, terminate and output $\mathbf{x}^{(i)}$ and $\mathbf{z}^{(i)}$; otherwise, return step 2.

4. Simulation

The simulation is provided to demonstrate the effectiveness of the proposed sequential iterative optimization algorithm. For each example, we select 10 available codes. The number of transmit antennas and receive antennas is $N=M=6$. The carrier frequency $f_0=9\text{GHz}$, d=0.0167cm. We choose $\delta=10^{-3}$ and $i_{\max}=8$.

Simulation 1: In this section, we consider four interference signals impinging the array. The angles of interference signals are $12^\circ, 15^\circ, 28^\circ, -28^\circ$. The angle of desired signal is 10°. We set INR=50dB, SNR=20dB.

Figure 2 shows the output F versus the iteration number. We find that the F converges quickly with the proposed sequential iterative optimization algorithm.

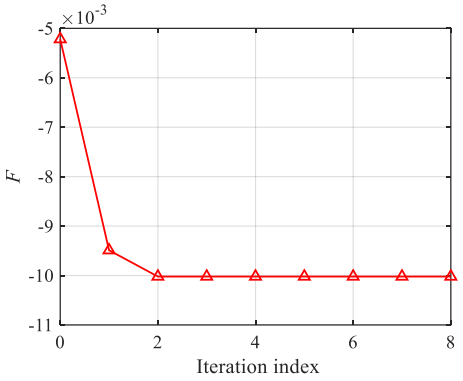

Fig. 2 Algorithm convergence

Simulation 2: We consider SINR and CRLB under various Pareto Weights, μ. Figure 3 shows the SINR and CRLB with various Pareto Weights. In Figure 3 (a), as the Pareto weight increases, SINR shows a downward trend. However, we can see that as the Pareto weight increases, CRLB shows a downward trend in Figure 3 (b). According to the definition of the objective function, as the Pareto weight value increases, the weight in the objective function increases, and the SINR decreases.

Moreover, high SINR and low CRLB can not be obtained simultaneously. We can only obtain appropriate results by adjusting the value of μ. To balance the SINR and CRLB, this paper sets the Pareto weight $\mu=0.5$.

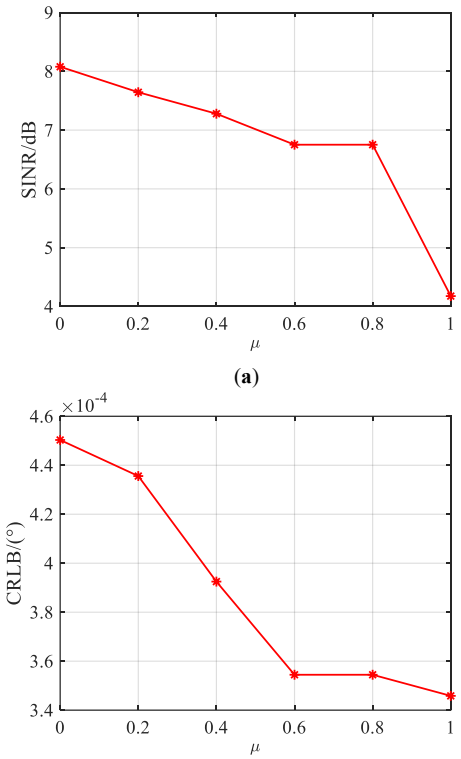

Fig. 3 Radar Performance with various Pareto Weights. (a) SINR (b) CRLB.

Simulation 3: This section considers SINR and CRLB optimization with various SNRs. We compare the proposed method with the other two cases. Case 1 is the method of [16], and case 2 is only waveform optimization with a fixed uniform selection vector. The Pareto Weight is 0.5 in all cases. The SNR range is 10~30dB. Figure 4 shows the SINR and CRLB with various SNRs. In Figure 4 (a), we can see that the average SINR of the proposed method is 6.95dB. The average SINR of case 1 and case 2 are 4.87dB and 1.51dB. The SINR of the proposed method is higher than case 1 and case 2 with various SNRs. As shown in Figure 4 (b), we can see that the average CRLB of the proposed method is $8.26\times10^{-4}(^\circ)$. Moreover, the average CRLB of case 1 and case 2 are $2.44\times10^{-3}(^\circ)$ and $1.37\times10^{-3}(^\circ)$. The optimization result of the proposed method is better than other cases.

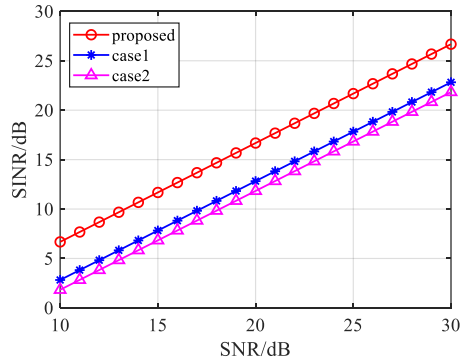

(a)

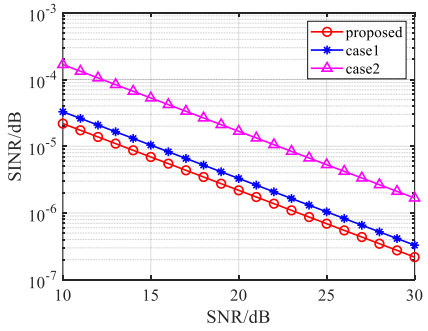

(b)

Fig. 4 Radar Performance with various SNR. (a) SINR (b) CRLB.

Simulation 4: In actual environments, the target usually maneuvers in the air, resulting that the angle of target is various. The proposed method is also applicable to target various angle. This section considers SINR and CRLB optimization with various desired echo signal angles. We will prove the advantage of the proposed sequential iterative optimization algorithm for various angles. We also compare the proposed method with the other two cases. In the simulation, the angle is $-80^\circ \sim 80^\circ$. Figure 5 shows the SINR and CRLB with target angles, $-80^\circ \sim 80^\circ$. In Figure 5 (a), the average SINR of the proposed method is 16.23dB. Furthermore, the average SINR of case 1 and case 2 are 14.06 dB and 11.01dB. We can see that the SINR of the proposed method is higher than case 1 and case 2 with various angles. It proves that the proposed method can better suppress interference. In Figure 5 (b), the average CRLB of the proposed method is $6.23\times10^{-4}(^\circ)$. The average CRLB of case 1 and case 2 are $1.02\times10^{-3}(^\circ)$ and $2.13\times10^{-3}(^\circ)$. We can see the CRLB of proposed method is lower than case 1 and case 2 with various angles. The proposed method has better theoretical estimation accuracy. By comparing and analyzing, we can conclude that the radar has better performance with optimized array parameters with proposed method.

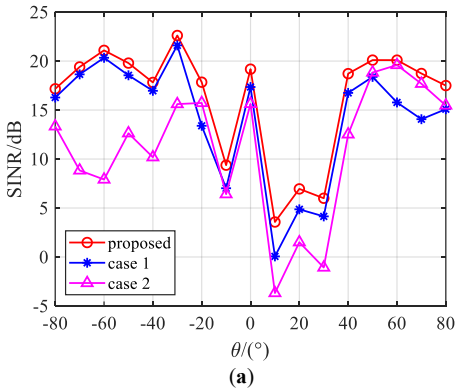

(a)

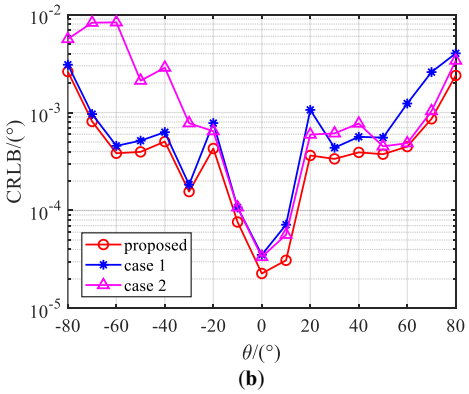

Fig. 5 Radar Performance with various angle. (a) SINR (b) CRLB.

5. Conclusions

In this paper, we proposed a sequential iterative optimization algorithm with thinned waveform code to obtain better performance. Firstly, we derive the relationship with SINR, CRLB, and waveform code **x**, waveform code-antenna selection **z**, respectively. Then, to better evaluate MIMO radar performance, we introduce Pareto weight to combine SINR and CRLB. We can get a new function that represents radar performance. We establish optimization problems for the performance to improve radar performance with the new function. Under waveform and selection vector constraints, the optimization problem is a multivariate non-convex problem. We proposed a sequential iterative optimization algorithm. We decompose the problem into two subproblems about **x** and **z**. For optimization of **z**, we transform the optimization problem into a conventional convex optimization problem by logarithms and first-order Taylor expansions. For optimization of **x**, we introduced an auxiliary variable and solved it by ADMM. The CVX toolbox can solve both subproblems. Finally, the simulation experiment shows that the proposed method can obtain the higher SINR and lower CRLB than in other cases. We can obtain better MIMO radar performance and low array complexity.

Acknowledgments

This research was funded by the National Nature Science Foundation of China, grant number 62201580; The Program of the Youth Innovation Team of Shanxi Universities.

References

[1] E. Fishler, A. M. Haimovich, R. S. Blum, L. Cimini, D. Chizhik, and R. A. P. o. t. I. R. C. Valenzuela, "MIMO radar: an idea whose time has come," pp. 71-78, 2004.

[2] J. Li and P. Stoica, "MIMO Radar Diversity Means Superiority," 2009.

[3] B. Hu, X. C. Wu, X. Zhang, Q. Yang, D. Yao, and W. B. Deng, "Adaptive Beamforming Based on Compressed Sensing with Gain/Phase Uncertainties," IEICE Trans. Fundamentals, vol. E101A, no. 8, pp. 1257-1262, Aug 2018.

[4] X. Y. Luo, X. C. Fei, L. Gan, P. Wei, and H. S. Liao, "Direction-of-arrival estimation using an array covariance vector and a reweighted," IEICE Trans. Fundamentals, vol. E98A, no. 9, pp. 1964-1967, Sep 2015.

[5] W. H. Lv, L. H. Hu, W. J. Zeng, H. L. Wang, and Z. K. Luo, "JointWideband Spectrum and DOA Estimation with Compressed Sampling Based on L-Shaped Co-Prime Array," IEICE Trans. Fundamentals, vol. E105A, no. 7, pp. 1028-1037, Jul 2022.

[6] A. H. Shaikh, X. Y. Dang, I. A. Khoso, and D. Q. Huang, "Three-Stage Padding Configuration for Sparse Arrays with Larger Continuous Virtual Aperture and Increased Degrees of Freedom," IEICE Trans. Fundamentals, vol. E105A, no. 3, pp. 549-561, Mar 2022.

[7] Y. Tian, Q. S. Lian, and K. Liu, "2-D Angles of Arrival Estimation Utilizing Two-Step Weighted l_1-Norm Penalty under Nested Coprime Array with Compressed Inter-Element Spacing," IEICE Trans. Fundamentals, vol. E100A, no. 3, pp. 896-901, Mar 2017.

[8] Y. Doi *et al.*, "High Resolution 2-D DOA Estimation by Low-Cost Antenna Array Based on Synthesized Covariance Matrix via Antenna Switching," IEICE Trans. on Fundamentals, vol. E96A, no. 10, pp. 1962-1971, Oct 2013.

[9] P. Pal and P. P. Vaidyanathan, "Nested Arrays: A Novel Approach to Array Processing With Enhanced Degrees of Freedom," IEEE Trans. Signal Processing, vol. 58, pp. 4167-4181, 2010.

[10] A. Ahmed and Y. D. Zhang, "Generalized Non-Redundant Sparse Array Designs," IEEE Trans. on Signal Processing, vol. 69, pp. 4580-4594, 2021.

[11] Z. Zheng, M. Fu, W.-q. Wang, and H. Cheung, "Symmetric Displaced Coprime Array Configurations for Mixed Near- and Far-Field Source Localization," IEEE Trans. Antennas Propagation, vol. 69, pp. 465-477, 2021.

[12] S. Junpeng, W. Fangqing, L. Yongxiang, L. Tianpeng, and L. Zhen, "High-order extended coprime array design for direction of arrival estimation," Journal of Systems Engineering Electronics, 2021.

[13] X. Wang, M. G. Amin, and X. Cao, "Analysis and Design of Optimum Sparse Array Configurations for Adaptive Beamforming," IEEE Trans. Signal Processing, vol. 66, pp. 340-351, 2018.

[14] X. Wang, M. S. Greco, and F. Gini, "Adaptive Sparse Array Beamformer Design by Regularized Complementary Antenna Switching," IEEE Trans. Signal Processing, vol. 69, pp. 2302-2315, 2021.

[15] Z. Zheng, Y. Fu, and W.-q. Wang, "Sparse Array Beamforming Design for Coherently Distributed Sources," IEEE Trans. Antennas Propagation, vol. 69, pp. 2628-2636, 2021.

[16] X. Wang, E. Aboutanios, and M. G. Amin, "Slow radar target detection in heterogeneous clutter using thinned space-time adaptive processing," IET Radar Sonar Navigation, vol. 10, pp. 726-734, 2016.

[17] X. Wang, W. Zhai, M. S. Greco, and F. Gini, "Cognitive Sparse Beamformer Design in Dynamic Environment via Regularized Switching Network," IEEE Trans. Aerosp. Electron. Syst., vol. 59, pp. 1816-1833, 2023.

[18] N. K. Chen, P. Wei, L. Gao, H. G. Zhang, and H. S. Liao, "Joint Design of Transmitting Waveform and Receiving Filter for Colocated MIMO Radar," IEICE Trans. Fundamentals, vol. E105A, no. 9, pp. 1330-1339, Sep 2022.

[19] L. Shen, J. H. Wang, W. Guo, and R. Luo, "Doppler Resilient Waveforms Design in MIMO Radar via a Generalized Null Space Method," IEICE Trans. Fundamentals, vol. E105A, no. 11, pp. 1503-1507, Nov 2022.

[20] W. Z. Yue, Y. Zhang, and J. W. Xie, "Radar Constant-Modulus Waveform Design for Multiple Extended Targets," IEICE Trans. Fundamentals, vol. E100A, no. 3, pp. 888-892, Mar 2017.

[21] W. Yuxi, H. Guoce, and L. Wei, "Waveform design for radar and extended target in the environment of electronic warfare," Journal of Systems Engineering Electronics, vol. 29, pp. 48-57,

2018.

[22] A. R. Chiriyath, S. Ragi, H. D. Mittelmann, and D. W. Bliss, "Radar Waveform Optimization for Joint Radar Communications Performance," Electronics, vol. 8, p. 1498, 2019.

[23] J. Hu, W. Zhang, W. Xiong, K. Zhong, Z. Wei, and L. Yuzhi, "Constant modulus waveform design for MIMO radar via manifold optimization," Signal Processing, 2022.

[24] S. Lu, G. Cui, X. Yu, L. Kong, and X. Yang, "Cognitive Radar Waveform Design Against Signal-Dependent Modulated Jamming," Progress in Electromagnetics Research B, vol. 80, pp. 59-77, 2018.

[25] S. Wang, Z. Liu, R. Xie, L. Ran, and J. Wang, "MIMO radar waveform design for target detection in the presence of interference," Digit. Signal Process., vol. 114, p. 103060, 2021.

[26] L. L. Wu, P. Babu, and D. P. Palomar, "Transmit Waveform/Receive Filter Design for MIMO Radar With Multiple Waveform Constraints," Ieee Transactions on Signal Processing, vol. 66, no. 6, pp. 1526-1540, Mar 2018.

[27] X. Zhang, X. Wang, and X. Wang, "Joint antenna selection and waveform design for coexistence of MIMO radar and communications," EURASIP Journal on Advances in Signal Processing, vol. 2022, pp. 1-27, 2022.

[28] E. Tohidi, M. Coutiño, S. P. Chepuri, H. Behroozi, M. M. Nayebi, and G. Leus, "Sparse Antenna and Pulse Placement for Colocated MIMO Radar," IEEE Trans. Signal Processing, vol. 67, pp. 579-593, 2018.

[29] A. Bose, S. Khobahi, and M. Soltanalian, "Efficient waveform covariance matrix design and antenna selection for MIMO radar," Signal Process., vol. 183, p. 107985, 2020.

[30] C. x. Chu, Y. Chen, Q. Zhang, and Y. Luo, "Joint linear array structure and waveform design for MIMO radar under practical constraints," Electronic Research Archive, 2022.

[31] Y. Liu, C. Pan, X. Liu, Y. Zhu, and Y. Liu, "A Waveform Design for MIMO Sensing on Two-Dimensional Arrays with Sparse Estimation," Electronics, 2023.

[32] S. D. Blunt, E. J. I. A. Mokole, and E. S. Magazine, "Overview of radar waveform diversity," vol. 31, pp. 2-42, 2016.

Mingjie Liu was born in Tianjin, China, in 1997. He received the B.S. and M.S. degrees from the Air Force Engineering University, Xi'an, China, in 2019 and 2021, respectively, where he is currently pursuing the Ph.D. degree. His research interests include array signal processing and radar anti-jamming.

Chunyang Wang was born in 1967. He received his M.S. and Ph. degree in the electromagnetic field and microwave technique from the Air Force Engineering University, Xi'an, China, in 1991 and 2004, respectively. He is currently a Professor at the Air and Missile Defense College, Air Force Engineering University. His current research interests include radar signal processing, radar jamming, and anti-jamming technologies.

Jian Gong was born in Shandong, China, in 1984. In 2018, he received his Ph. degree from Xidian University. He is currently an associate professor at the Air Force Engineering University. His research interests include Radar electronic warfare signal processing technology.

Ming Tan was born in Sichuan, China, in 1992. In 2020, he received his Ph. degree from the Air Defense and Missile Defense College of Air Force Engineering University. He is currently a lecturer at the School of Information and Communication, National University of Defense Technology. His research interests include frequency diverse arrays and radar anti-jamming methods.

Changlin Zhou was born in Sichuan, China, in 1997. In 2019, he received his B.S. degree from the Air Defense and Missile Defense College of Air Force Engineering University. His research interests include frequency diverse arrays and radar anti-jamming methods**.**